LOOP SEPARATION BASED CONTROLLER APPLIED ON A MISSION OF A HIGHLY FLEXIBLE AIRCRAFT

PEDRO J. G. RAMÍREZ

Aerospace Engineering Division, Instituto Tecnológico de Aeronáutica
São José dos Campos, SP, 12228-900
E-mails: pgonzalez@ita.br

FLÁVIO J. SILVESTRE[1], PEDRO PAGLIONE[1], RAFAEL M. BERTOLIN[1], ZI YANG PANG[2], AND CARLOS E. S. CESNIK[2]

Aerospace Engineering Division, Instituto Tecnológico de Aeronáutica[1],
Department of Aerospace Engineering, University of Michigan[2]
São José dos Campos, SP, 12228-900[1], Ann Arbor, MI, United States, 48109-2410[2]

E-mails: flaviojs@ita.br, pedro.paglione@gmail.com, rafaelmbufsj@gmail.com, pziyang@umich.edu, cesnik@umich.edu

Abstract— This research evaluates the capability of the loop separation control designed for the experimental aircraft X-HALE to complete a typical HALE mission pattern. The loop separation is a new approach in control design for highly flexible aircraft; it consists in two control loops. An inner loop capable of controlling the shape of the aircraft while it keeps the plant stable. The outer loop is designed using non-smooth optimization techniques to control rigid body states for commanded speed, sideslip, heading and altitude. The controller is efficient for completing the flight pattern with low control energy and inside the maneuver requirements while holding the wing strains at a low level.

Keywords— control of flexible aircraft, loop separation control, aircraft control, autopilot.

Resumo— Esta pesquisa avalia a capacidade do controle por separação de malhas projetado para a aeronave experimental X-HALE numa missão HALE padrão. A separação de malhas é uma nova abordagem em projeto de controladores para aeronaves muito flexíveis; consiste em duas malhas de controle: uma malha interna capaz de controlar a forma da aeronave enquanto mantem o sistema estável; e uma malha externa projetada utilizando técnicas de otimização não suave para controlar os estados de corpo rígido para comandar a velocidade, o ângulo de derrapagem, o rumo e a altitude. O controlador é capaz de completar o voo padrão com baixa energia de controle e respeitando os principais requisitos de manobra enquanto a malha interna suprime a deformação das asas.

Palavras-chave— controle de aeronaves flexíveis, controle por separação de loops, controle de aeronaves, auto piloto.

1 Introduction

The development of new technologies and new goals in aeronautical industry has impulsed the evolution of a new generation of aircraft. The High Altitude Long Endurance (HALE) vehicles are the solution to the necessity of suborbital flights to assist the crescent demand in radio transmissions, atmospheric research, surveillance, reconnaissance and research. (Cesnik, 2014).

For the past 30 years, research effort has helped to improve the capabilities of HALEs, from unmanned examples like the Helios (Noll, 2006) or the Zephyr (Davey, 2007) to manned vehicles like the Solar Impulse 2 currently making its first flight around the world. All these aircraft share same characteristics of having high aspect ratio flexible wings.

The increase of the wing aspect ratio helps to increase aerodynamic efficiency. Which means that there exists greater lift to drag ratio causing a reduction of fuel consumption. It also makes necessary to enhance the structural efficiency. This is required to keep the structure as light as possible, however it must be capable to hold maneuvers and gust loads. Composite materials are often offered as a solution for this structural solicitation, but they result in nonlinearities in the structural behavior (Cesnik, 2014).

The mass reduction on the aircraft structure produces a decrease in stiffness of the wing and an increase in flexibility. The increase of flexibility has a direct effect in the flight dynamics of an aircraft; the rigid body modes of the airplane get closer in frequency to the vibration modes of the structures. The model could couple inducing limit cycle oscillation or even flutter.

HALE's missions are usually designed to be long term, which require control efficiency to ensure autonomous operation with little or without human intervention. Control laws installed on the aircraft must be able to adapt to different flight patterns and atmospheric conditions. The control law has to be implemented on board the aircraft. This means that simplicity of the controller is a requirement of the control project (Nickol, 2007).

A typical HALE mission profile is shown in Figure 1. The vehicle takes off, then it climbs to the transit altitude at optimum speed, then it travels to the mission area. Once it gets to the observation point, it starts a reconnaissance flight around the target. When the observation time has finished, the airplane returns to the base at its optimum transit altitude and speed, descent and land (Nickol, 2007).

Normally, control laws are designed based in the rigid body approximation of the aircraft flight dynamics. The flexibility of the wing changes the flight dynamics characteristic of the aircraft, which makes this approximation invalid.

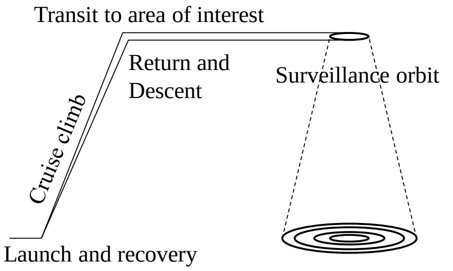

Figure 1. Typical HALE mission profile

Since 2011, the Active Aeroelasticity and Structures Research Laboratory of the University of Michigan (UMich) has been developing X-HALE, an experimental representative highly flexible aircraft. This is a radio-controlled testbed used to validate structural models, to study flexible aircraft flight dynamics and lately in cooperation with Laboratory of New Concepts in Aeronautics (LNCA) of Instituto Tecnológico de Aeronáutica new flight control laws.

Recently, a linear control of highly flexible aircraft based on loop separation has been developed to guarantee control and maneuverability of the X-HALE (González, 2016). The objective of the work presented herein is to evaluate the capability of this control architecture to complete a typical HALE mission pattern.

2 X-HALE: Description and numerical model

X-HALE is a radio-controlled aircraft with 6 m wingspan and a wing chord of 0.2 m. The outer panels of the wing have a dihedral of 10 degrees. It has five pods distributed equidistantly on the wing, tail booms are linked to these pods holding the stabilizers; the aircraft has three ventral fins on the central pods to increase lateral stability. Pods contain engines and instrumentation (Cesnik, 2012). Figure 2 presents the X-HALE.

X-HALE Aeroelastic Test Vehicle (ATV) is the full-instrumented version of the X-HALE. This testbed uses a camera system to measure the deformation of the wing in flight. The cameras are installed on the central pod facing outwards as seen in Fig. 2. Wings have a set of three pairs of LED (light emitting diode) markers on each panel. The camera system is capable to detect the variation of vertical displacement of the markers. During post-processing is possible to obtain the deflection of the wing. The objective of this platform is to offer information to validate coupled models of flight and aeroelastic dynamics and control laws for flexible aircraft (Pang, 2014).

X-HALE is unstable in dutch roll when the movable central fin is flipped horizontally. Because of the risk involved in the operation of the aircraft, Risk Reduction Vehicle (RRV) was projected. This is a lightly instrumented platform to familiarize the pilot and understand the flight behavior of the aircraft. The model used in this research represents the RRV.

Structure is modelled using two flexible elements for each of the inboard one-meter panels. The outboard panels are modelled with four flexible elements. Horizontal stabilizers have two elements each. Booms, tails and central pods are modelled using rigid elements. Wings, fins and stabilizers represent the lifting surfaces on the aerodynamic model, while booms are modelled as non-lifting surfaces.

The linearized model of the X-HALE is of the form

$$\dot{x} = Ax + Bu \qquad (1)$$
$$y = Cx + Du$$

A is the state matrix with 344 states. *B* is the input matrix, *C* the output matrix, *x* is the state vector, *y* is the control output, *u* is the control input. The state vector includes structural strains, rigid body motion states and aerodynamic inflow states. It is defined as

$$x = \begin{bmatrix} \varepsilon_n & \dot{\varepsilon}_n & \beta_M & \zeta & P_G & \lambda_m \end{bmatrix}^T \qquad (2)$$

There are four degrees of freedom for each element of the structure, ε_n is a 4n by 1 vector where *n* is the number of flexible elements, containing axial strain ε_x and three orthogonal curvatures κ_x, κ_y and κ_z.

$$\varepsilon_{ni} = \begin{bmatrix} \varepsilon_x & \kappa_x & \kappa_y & \kappa_z \end{bmatrix}^T \qquad (3)$$

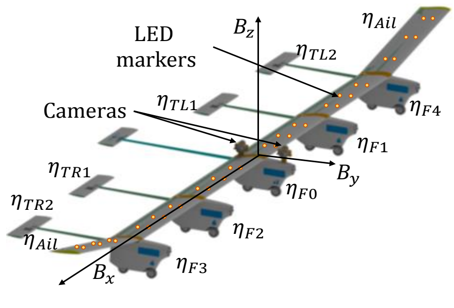

Figure 2. X-HALE with axes and control identification

The structural reference axis *x* is in the direction of the wing spam, *y* is chord wise and *z* completes the axes, it is positive upwards. β_M includes the body rotation rates in the body frame and three-axis body rates. P_G is the position vector in the inertia frame. There are six inflow associated states with each lifting surface, represented by λ_m.

Five control surfaces (horizontal stabilizers, $\eta_{TR1\text{-}2,\ TL1\text{-}2}$ and ailerons η_{Ail}) and five engines ($\eta_{F0\text{-}4}$) give the control input of the X-HALE, as is seen in Fig. 2.

The operation limits of the control surfaces are ±30 degrees. The model of the engine is in function of throttle and aircraft speed. For the nominal speed of 14 m/s the maximum thrust of the engine is approximately 5 N.

The control input vector is

$$u = [\eta_{TL1} \quad \eta_{TR1} \quad \eta_{TL2} \quad \eta_{TR2} \quad \eta_{Ail} \quad \eta_{F0} \quad \eta_{F1} \quad \eta_{F2} \quad \eta_{F3} \quad \eta_{F4}]^T \tag{4}$$

3 Loop Separation Architecture

Loop separation concept consists in an inner loop in charge of stabilizing the flexible aircraft and an outer loop for navigation (González, 2016). The inner loop must ensure that all poles be on the left side of the imaginary axis, while resulting in damped response in the time-domain at low control energy. The high level of deformation and deformation rate has a huge influence on the flight dynamics of an aircraft. The inner loop has then the task to keep the steady-state shape of the aircraft while maneuvering or in face of external disturbances.

The outer-loop is designed with a conventional compensator approach. The compensators were used to generate the command inputs for height h, velocity V, sideslip β and heading angle tracking ψ. Heading reference is attained commanding a bank angle ϕ. The control law architecture of X-HALE is shown in Figure 3.

3.1 Inner loop

The inner loop is basically a proportional controller acting over measured outputs, which are: pitch angle θ, angular rates p, q and r, and strains at all six panels. The measured strains are torsion and bending strains on the center of each panel.

The control inputs of the inner loop are the two central stabilizers actuated together for longitudinal control and the outer elevators and the ailerons for lateral-directional and structural control

Proportional gains have been scheduled using Linear Quadratic Regulator (LQR) approach, with output feedback.

The LQR problem consists in finding a feedback coefficient matrix K, that given a linear system of Eq. 1 and a control signal $u = -Ky$, minimizes the magnitude of the performance index J_{lqr} (Stevens, 2003).

$$J_{lqr} = \frac{1}{2}\int_0^{\infty}\left[x^T Q x + u^T R u\right]dt \tag{5}$$

Introducing the control signal expression in Eq. 1, the close loop system A_c is obtained

$$\dot{x} = (A - BKC)x \equiv A_c x \tag{6}$$

The conditions to solve the LQR problem with output feedback are given by two Lyapunov equations and a third equation to obtain K (Stevens, 2003).

$$0 = A_C{}^T P + PA_c + Q - PBR^{-1}B^T P \tag{7}$$

$$0 = A_c S + SA_C^T + X \tag{8}$$

$$K = R^{-1}B^T PSC^T (CSC^T)^{-1} \tag{9}$$

To obtain the gain that minimizes the performance index J_{lqr}, it is necessary to solve the three coupled equations. This makes the solution only iteratively possible.

If the system is stable, the performance index of Eq. (5) can be written as

$$J_{lqr} = \frac{1}{2}x^T(0)Px(0) = \frac{1}{2}tr(PX) \tag{10}$$

After a stabilizing gain is found minimizing the maximum real part of the eigenvalues of A_c until it gets negative, Equation (7) is solved iteratively. The algorithm would use Eq (7) and Eq. (10). For a given value of K, the Lyapunov equation is solved for P and then use P in Eq. (10) to determine J_{lqr}. It must vary the elements of K to minimize J_{lqr}.

The inner loop of X-HALE is presented inside the red square of Fig. 3. The final gain matrix has a dimension of 4 by 16 and it is completely coupled.

3.2 Outer-loop

Outer-loop of this control system is in charge of tracking commanded velocity, heading, sideslip angle and altitude. The architecture of the outer-loop is comparable to a classical multivariable approach for aircraft control design (Stevens, 2003). This approach allows defining control gains that minimize a performance index over the enclosed structure. The tracking command acts over the system described in Eq. 1. The performance output is.

$$z = Hx \tag{11}$$

The state of the compensator is $w(t)$ and the respective command of the outer loop *is* $u_v(t)$. The

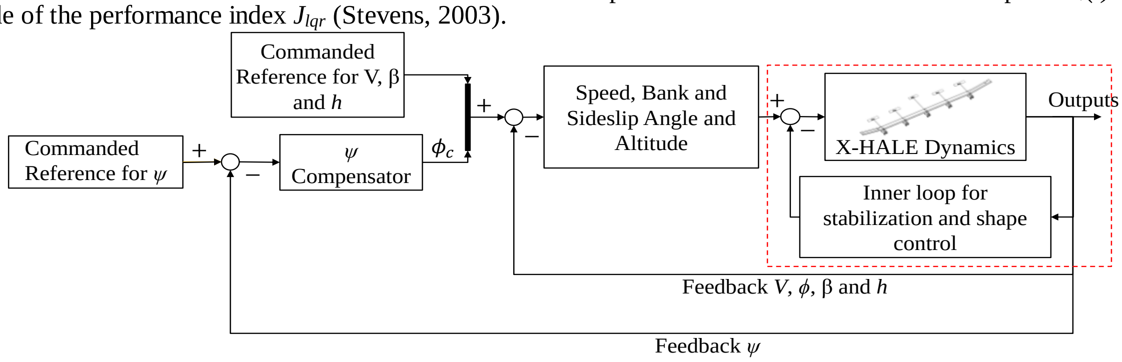

Figure 3. Structure for the control system of the X-HALE

compensator dynamics is

$$\dot{w} = Fw + Ge \quad (12)$$
$$u_v = Dw + Je$$

The reference is denoted as *r(t)* and the tracking error is defined as

$$e(t) = r(t) - z(t) \quad (13)$$

Total control input to the plant is a sum of the inner loop and outer loop actions,

$$u = -Ky - u_v \quad (14)$$

The augmented system is

$$\frac{d}{dt}\begin{bmatrix} x \\ w \end{bmatrix} = \begin{bmatrix} A & 0 \\ -GH & F \end{bmatrix}\begin{bmatrix} x \\ w \end{bmatrix} + \begin{bmatrix} B \\ 0 \end{bmatrix}u + \begin{bmatrix} 0 \\ G \end{bmatrix}r \quad (15)$$
$$\begin{bmatrix} y \\ u_v \end{bmatrix} = \begin{bmatrix} C & 0 \\ -JH & D \end{bmatrix}\begin{bmatrix} x \\ w \end{bmatrix} + \begin{bmatrix} 0 \\ J \end{bmatrix}r$$
$$z = \begin{bmatrix} H & 0 \end{bmatrix}\begin{bmatrix} x \\ w \end{bmatrix}$$

The control input is

$$u = -\begin{bmatrix} K & I \end{bmatrix}\begin{bmatrix} y \\ u_v \end{bmatrix} \quad (16)$$

Equations 15 allow to include the dynamics of the compensator in Eq.1.

$$\dot{x}_a = Ax_a + B_a u_a + Gr$$
$$y_a = Cx_a + Fr \quad (17)$$

x_a is the augmented states considering the states of the compensator. The objective of the optimization process is to define the matrices *F*, *G*, *D* and *J* to attain the references. This calculation is completed by closing all loops at the same time. The close-loop system is

$$\dot{x} = (A - BKC)x_a + (G - BIF)r \quad (18)$$

This optimization process was accomplished by fixed structure techniques. Fixed structure is a technique that uses non-smooth optimizers with design requirements as H_∞ constraints in order to provide a solution usually comparable to a full order H_∞ synthesis solution. One of the benefits of this method is the straightforwardness and order of the structure (Bompart, 2007).

Apkarian (2014) states that the structure of this problem matches the form of a traditional H_∞ problem. *PG* is the description of open loop plant in a state space form. State vector is $x_a \in \mathbb{R}^{np}$, exogenous input vector is $e \in \mathbb{R}^{nw}$, $u \in \mathbb{R}^{nu}$ is the control input vector and K_{ext} is feedback controller. Regulated output vector is $z \in \mathbb{R}^{nz}$ and the measured output is $y \in \mathbb{R}^{ny}$. Equation 18 shows typical representation of *PG(s)*

$$PG: \begin{cases} \dot{x}_a = Ax_a + B_a u_a + Gr \\ z = Hx_a \\ y_a = Cx_a + Fr \end{cases} \quad (19)$$

$$K_{ext}: \begin{cases} \dot{w} = Fw + Ge \\ u_v = Dw + Je \end{cases} \quad (20)$$

K_{ext} is the feedback controller with $x_k \in \mathbb{R}^{nk}$, and is called structured if the matrices F_k, D_k, G_k, J_k depend smoothly on a design parameter $x \in \mathbb{R}^n$.

The optimization of the gains for the outer-loop of the X-HALE was done with Systune a modern control tool available in the Matlab Robust Control System Toolbox.

The objective of the optimization algorithm is to tune the parameters of Eq. 20 to enforce the closed loop stability. Systune solves a multi objective constrained optimization problem with soft and hard constraints of the form

$$\begin{aligned} \text{minimize} \quad & f(x) = \max_{k \in SOFT, i \in I_K} \left\| T_{eizi}^{(k)}(K(x)) \right\| \\ \text{subject to} \quad & g(x) = \max_{k \in HARD, j \in I_K} \left\| T_{ejzj}^{(k)}(K(x)) \right\| \le 1 \\ & K_{ext}(x) \text{ structured and stabilizing} \end{aligned} \quad (21)$$

T is the cosensitivity function. The notation $T_{e \to z}$ is used to represent the closed-loop map from signal *e* to signal *z*. The goal of Eq. 21 is to minimize the worst-case cost of the soft constraints while enforcing the hard constraints and close loop stability (Apkarian, 2014).

Design requirements of the controller are based on the ability of the aircraft to attain the commanded reference, while all the requirements of the inner loop are kept. An iterative process was developed to construct a proper controller. Constrains were applied on PK_{ext} functions, the open loop cut off frequency were set between 0.25 and 1 rad/sec to reach the physical limit of the aircraft actuators, the constraints were tight until the optimization process was capable to reach the desired performance

A four-controller configuration was proposed for the X-HALE. Two central elevators give control input for the velocity controller. The bank angle is controlled with the two outer elevators acting together differentially. The sideslip angle is regulated with the differential thrust of the outer engines acting a pair minus the other, height is commanded with the five engines together. The structure of the control input for the outer loop is

$$\begin{aligned} u_a = [&\eta_{TR2} + \eta_{TL1} \quad \eta_{TR4} - \eta_{TL2} \\ &\eta_{F2} + \eta_{F3} - (\eta_{F1} + \eta_{F4}) \\ &\eta_{F0} + \eta_{F1} + \eta_{F2} + \eta_{F3} + \eta_{F4}]^T \end{aligned} \quad (22)$$

Case of study

Case of study consists in a typical HALE mission pattern for X-HALE with control architecture previously described. The aircraft must take off from the track and then ascend to 30 m. Once the commanded altitude is reached, the aircraft must fly leveled to the target. It must complete an orbital pattern over the target, the radius of the turn is 275 meters, finally it returns to the departure area and land.

Figure 4 shows the resultant maneuver for the commanded inputs mentioned before. The entire mission last 284 seconds and X-HALE completed two loops over the target.

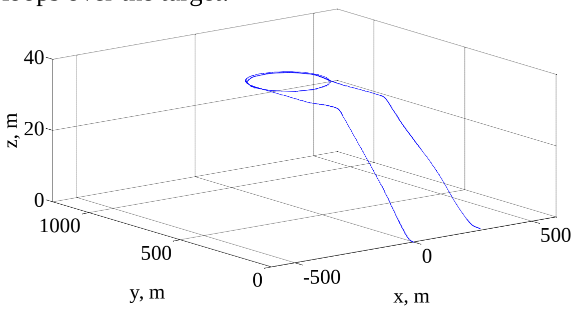

Figure 4. Mission profile completed by the X-HALE

Figures 5 presents velocity, heading and sideslip angle tracked by the outer loop.

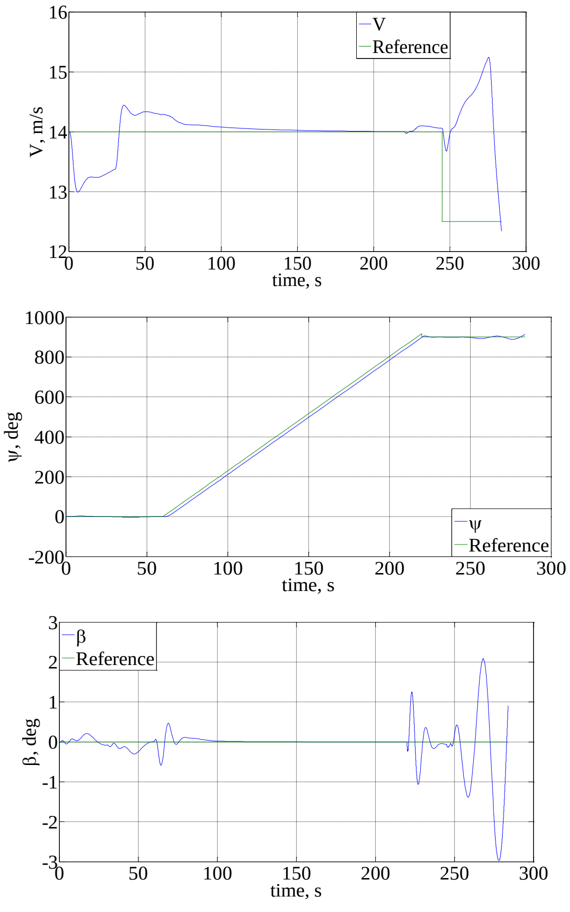

Figure 5. Tracked signals by the outer loop

The aircraft takes off when it reaches 14 m/s. Due to the increase of altitude the aircraft loses velocity. The controller is continuously trying to compensate this reduction of speed until X-HALE reaches the operation height. Once the aircraft has reached the 30 m height, the velocity is regained and held. Velocity has no major variation during turn, and is kept with a small error with respect to the reference. Once the aircraft starts the descent it is possible to observe and increase in speed. At the same time, the aircraft is commanded to reduce velocity to 12 m/s. The controller is capable to reduce the aircraft velocity at the end of the mission.

Heading *(ψ)* is shown in Fig. 5. X-HALE is capable to keep the zero degree orientation commanded by the reference. When X-HALE reaches the target area, it completes the orbital pattern performing two and a half laps over it. Once the observation has been completed, it returns to the landing area. It is possible to observe that the heading tends to increase the error during the final phase. While during the entire mission the maximum heading error was from +3 to – 3.5 degrees. During the landing phase the error increases to 10 degrees. This represents a 14-meter error respect the expected point of touch down. Nevertheless, during the rest of the mission the error was relatively small.

The sideslip angle was kept during the entire orbital pattern, actually during the turn the error was below 0.01 degrees. During the ascension the sideslip varies between -0.5 and 0.4 degrees. The greater error occurs again during the descent and landing when it grow between -2 and 2.9 degrees.

Figure 6 shows that altitude tracker is capable to ascend to the commanded height, the maximum overshoot is 3.3 % and the stationary state error is less than 1.5 %. Once the mission is finished, the aircraft is capable to descent and complete the landing

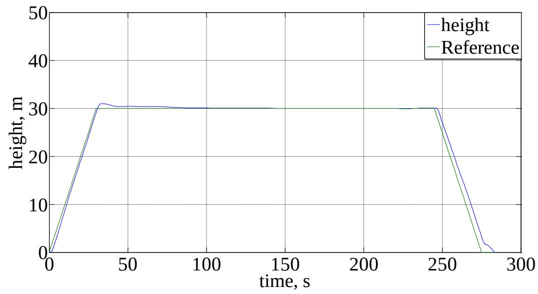

Figure 6. Altitude variation in time domain

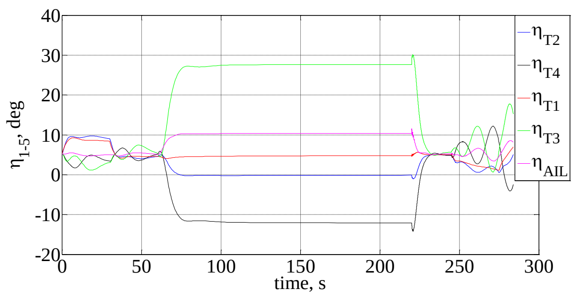

Figure 7. Control surface control inputs during simulation

The control input required to complete the mission is presented in Fig. 7 and Fig. 8. The control surfaces are keeping the shape of the wing and commanding the heading and speed tracking. Controls are capable to reach all commanded references without saturation. Once the reference is reached, the control surfaces and engines hold the level flight condition. The problem of heading and sideslip increasing during the landing could be addressed to the fact that the engines are dropping entirely to attain the commanded altitude.

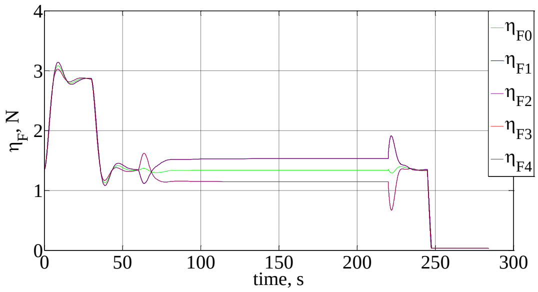

Figure 8. Engine thrust during simulation

Figure 9 shows the variation of bending strains during the entire flight and the correspondent deformation of the aircraft for different moments of the mission. It is possible to verify how the strains always tend to return to the equilibrium condition. The maximum level of the deformation is obtained during the turn (time steps 60 s and 150 s). After the turn phase, the strains tend to reduce and the aircraft shape is now closer to the trimmed shape, as it can be observed at the time step of 220 s. The strain level increases again during the landing, the lack of directional control makes the aircraft slips, which increase the deformation.

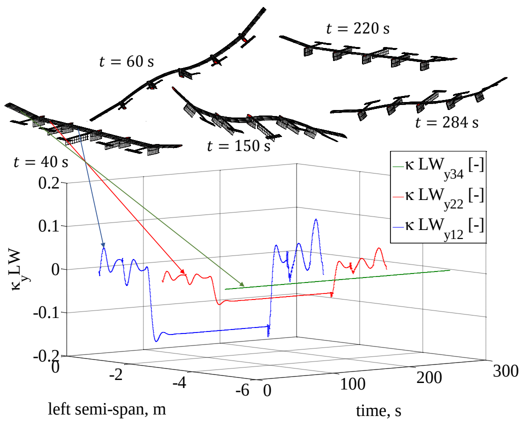

Figure 9. Variation of bending wing strain

Summary

The loop separation control proposed for the flexible aircraft X-HALE is capable to command the aircraft to complete a regular HALE flight pattern. This architecture consists in an inner loop capable of maintain the shape of the aircraft while ensure stability. The Outer loop is a fixed-structure controller; the gains and actuator bandwidth were optimized by a non-smooth technique. The commanded references were tracked satisfactorily. The loop separation concept shows promising results for its future implementation on board the platform. A landing control system must be designed for increasing appropriate tracking in this flight phase. It is common in this kind of project to perform robustness analysis, however in this work such approach was neglected because the objective of the research. In addition, nonlinearities introduced by variations in altitude during the case of study can be neglected.

Acknowledgment

The authors thank the financial support from the Brazilian funding agency Financiadora de Estudos e Projetos FINEP and EMBRAER.

References

Apkarian P., and Noll, D. (2014). Optimization-Based Control Design Techniques and Tools. Encyclopedia of Systems and Control, Springer London, pp. 1-12.

Bompart, V., Apkarian, P. and Noll, D., (2007). Non-smooth techniques for stabilizing linear systems. American Control Conference, WeB16.4, New York City, EEUU.

Cesnik, C., Senatore, P., Su, W., Atkins, E., Shearer, C., (2012). X-HALE: A Very Flexible Unmanned Aerial Vehicle for Nonlinear Aeroelastic Tests. AIAA Journal Vol. 50, No. 12, pp 2820-2833.

Cesnik, C., Palacios, R. and Reichenbach E., (2014). Reexamined Structural Design Procedures for Very Flexible Aircraft. Journal of Aircraft. Vol. 51, No. 5, pp 1580-1591.

Davey, P., (2007). Zephyr HALE UAS. AIAA Infotech Aerospace 2007 Conference and Exhibit, AIAA 2007-28467, Rohnert Park, California, EEUU.

González, P., Silvestre, F., Paglione, P., Köthe, A., Pang, Z., Cesnik, C., (2016). Linear Control of Highly Flexible Aircraft based on Loop Separation. AIAA Atmospheric Flight Mechanics Conference, Washington, EEUU.

Nickol, C., Guynn, D., Kohout, L., Ozoroski, T., (2007). High Altitude Long Endurance UAV Analysis of Alternatives and Technology Requirements Development. NASA/TP-2007-214861, Virginia, EEUU.

Noll,T.E.,Brown, J.M., Perez-Davis, M.E., Ishmael, S.D., Tiffany, G. C., and Gaier, M., (2004). Investigation of the Helios Prototype Aircraft Mishap. Vol. 1: Mishap Report [online article], http://www.nasa.gov/pdf/64317main_helios.pdf [retrieved 15 Oct. 2015].

Pang, Z., Cesnik, C. and Atkins, E., (2014). In-Flight Wing Deformation Measurement System for Small Unmanned Aerial Vehicles. 55th AIAA/ASMe/ASCE/AHS/SC Structures, Structural Dynamics, and Materials Conference AIAA SciTech 2014, AIAA 2014-0330, National Harbor, Maryland, EEUU.

Stevens, B. and Lewis, F., (2003). Aircraft control and simulation, John Wiley & Sons.